



Research Journal of  
**Environmental  
Sciences**

ISSN 1819-3412



Academic  
Journals Inc.

[www.academicjournals.com](http://www.academicjournals.com)



## Research Article

# Effects on Environmental Impact and Economics of Component Efficiencies for a Heating System with Seasonal Thermal Storage

S.J. Self, S. Koochi-Fayegh, M.A. Rosen and B.V. Reddy

Faculty of Engineering and Applied Science, University of Ontario Institute of Technology, 2000 Simcoe St. N. Oshawa, Ontario, L1H 7K4, Canada

### Abstract

**Background and Objective:** The use of intermittent thermal energy sources for heating, in combination with seasonal thermal energy storage, may be advantageous compared to conventional heating systems. The analysis of heating systems with seasonal thermal energy storage is complex, as there are many variables that potentially affect overall design and operation. The effects of subsystem characteristics on overall system economics and environmental impact are not fully understood at present. This study investigates how subsystem efficiencies, pipe losses and peak consumer load affect economics and carbon dioxide emissions. **Materials and Methods:** A method for analyzing the economic and environmental aspects of a heating system with seasonal thermal energy storage is developed and presented. The present study focuses on the influence of subsystem efficiency values and losses on system performance, rather than on detailed thermodynamic analyses. Values of subsystem efficiencies and thermal losses are varied within ranges reported in the literature. The system utilizes a solar thermal source, an underground thermal energy storage and a natural gas backup boiler, and is taken to serve a residential building in Ottawa, Canada. **Results:** The thermal supply piping and seasonal thermal energy storage are found to have the highest capital cost followed by the solar collectors and backup boiler. The consumer load has the greatest effect on economics and carbon dioxide emissions. The backup system efficiency has little effect on system economics due to the high solar fraction. **Conclusions:** The study provides insight into the importance of the characteristics of various subsystems of the system on its operation, cost and carbon dioxide emissions. The results and trends developed can aid design and feasibility studies. Future work is merited to analyze heating systems using alternative subsystem technologies.

**Key words:** Seasonal thermal energy storage, space heating, intermittent sources, solar thermal

**Citation:** S.J. Self, S. Koochi-Fayegh, M.A. Rosen and B.V. Reddy, 2017. Effects on environmental impact and economics of component efficiencies for a heating system with seasonal thermal storage. Res. J. Environ. Sci., 11: 5-17.

**Corresponding Author:** S.J. Self, University of Ontario Institute of Technology, 2000 Simcoe St. N. Oshawa, Ontario, L1H 7K4, Canada

**Copyright:** © 2017 S.J. Self *et al.* This is an open access article distributed under the terms of the creative commons attribution License, which permits unrestricted use, distribution and reproduction in any medium, provided the original author and source are credited.

**Competing Interest:** The authors have declared that no competing interest exists.

**Data Availability:** All relevant data are within the paper and its supporting information files.

## **INTRODUCTION**

The use of renewable energy resources, like solar radiation and wind, for heating is limited as they typically have intermittent production rates that may not coincide with building heating loads<sup>1</sup>. Thermal energy storage (TES) can reduce the effect of source intermittency and fluctuating heat demand<sup>2,3</sup>. Combining renewable energy resources with TES allows energy to be collected and stored until there is a demand, which could lead to more economic utilization of intermittent renewable and alternative energy sources<sup>4,5,2,6,3</sup>.

TES can be categorized by storage duration into short, medium and long-term. Short-term TES is used to assist in peak thermal loads and has storage lengths of hours up to a day<sup>7</sup>. Medium-term has a storage capacity from a day to a week. Long-term storage involves storage requirements from a week up to multiple months<sup>4</sup>. Long-term thermal storage can take advantage of seasonal climatic variations and is often referred to as seasonal thermal energy storage (STES)<sup>4,8,9,10</sup>. In northern climates, where seasonally varying space heating loads dictate energy consumption, STES can contribute significantly to intermittent thermal source integration for heat production<sup>11,6,9</sup>. A common use for STES is the storage of heat in the summer for space heating applications in the winter<sup>12</sup>.

Heating systems incorporating renewable energy sources, with STES, consist of five main subsystems: consumer, STES, intermittent/alternative source, backup source and thermal supply piping. The characteristics of each subsystem's affect the operation of the heating system. Effective integration of STES into heating systems requires detailed knowledge of subsystem operation and understanding of the interactions between subsystems.

Currently, limited work has been reported on the effects of intermittent/alternative and backup source characteristics, associated with a wide range of sources, on performance, economic and environmental aspects. Typically STES are custom built for the specific application and require detailed knowledge to conduct accurate performance, economic and environmental feasibility analyses. More information on the overall system design of heating systems with STES including the significance of subsystem parameters and interaction between subsystems would assist with the optimal integration into building applications and communities. Through investigating significant design considerations, it may be possible to develop accurate guidelines for use in basic and detailed system designs.

To help address these needs, a method to analyzing the economic and environmental aspects of a heating system with

STES is developed and presented here. To quantify the significance of subsystem parameters and the interaction between subsystems on system performance, parametric studies are conducted. The effects of varying consumer load, STES efficiency, intermittent source and backup source efficiency, supply network pipe losses on cost and CO<sub>2</sub> emissions are investigated.

## **MATERIALS AND METHODS**

A detailed thermodynamic analysis of heating systems with STES is not a significant focus of the present study. Rather, the influence of subsystem efficiencies and losses is of primary interest. Therefore, estimation of the subsystem efficiency and losses were assumed to be within the range of typical values found in the literature. The model is developed in such a fashion to allow for flexibility in analysis through independent variation in subsystem characteristics. Ideally, the interdependency of subsystem characteristics should be considered as variation of some characteristics may affect the choice of applicable subsystem technologies and range of operating conditions.

Information about consumer heating load and intermittent source availability are key characteristics in the analysis of heating systems with STES. RETScreen<sup>®13</sup> was used to determine the consumer load characteristics over the course of a year using the combined heat and power project template contained in the software. System location, building floor area and peak heating load of the building per unit of floor area were provided to the software. Values for total amount of thermal energy consumed annually, average rate of thermal energy consumption for each month and the peak rate of thermal energy consumption for the entire building space were returned. Ideally, consumer load characteristics would be determined using consumer load profiles developed through daily, hourly or minute by minute values. This method provides an approach to estimate consumer heating load characteristics using monthly averages. This limits the accuracy of the study since the heating load may vary considerably from the average values provided by the software.

Solar energy was taken as the intermittent source of heat production through the use of solar thermal collectors. RETScreen was used to determine the amount of thermal energy available for heat production using the solar power project template. System location, collector slope and solar azimuth were specified in the software and values of monthly average daily solar radiation per unit area on horizontal and tilted orientations were returned. The values were used for the thermodynamic analysis of the system.

**System description:** The proposed system model includes the main subsystems required for a heating system with STES including: consumer, intermittent energy source, STES, backup energy source and thermal supply piping. As a simplification, the model excludes auxiliary components typically found in heating systems such as heat pumps, pumps, heat exchangers, controls and monitoring devices. Exclusion of these auxiliary components may affect the accuracy of the results as the energy losses and consumption associated with their operation are excluded in the analysis.

The system considered is shown in Fig. 1. The energy is supplied to the consumer through an intermittent source supply chain and a backup source supply chain. In the intermittent source supply chain, energy is introduced to the system through the intermittent subsystem. The energy introduced to the system represents the amount of energy presented from the original intermittent energy source (amount of available solar irradiation). Heat is generated and transferred to the system through the intermittent source heat production subsystem and then split into two paths through pipe sections one and two. Pipe section one leads to the consumer for immediate use of the thermal energy. Whether the energy can be used immediately is dependent on the intermittent source production and consumer loads coinciding. When the rate of heat introduced to the system, by the intermittent source, exceeds the consumer load, it is directed through pipe section two and delivered to the STES subsystem. Heat is extracted from the STES and delivered to the consumer through pipe section three when the consumer load is higher than the supply through pipe section one.

A backup thermal energy source is included in the system to respond to the peak heating demands of the consumer and is contained in the backup source supply chain. Fuel is consumed (e.g., fossil fuel and electricity) by the backup subsystem and the thermal energy produced is delivered to the consumer through pipe section four.

**Analysis:** The following outlines the assumptions, equations and other relations and expressions that are used to perform thermodynamic, economic and environmental analyses of the system in Fig. 1.

The following assumptions are invoked to simplify the analysis and to assist in developing the governing relations:

- At the end of every annual cycle, the amount of energy stored in the STES system returns to the equivalent amount stored at beginning of the cycle (no annual thermal accumulation)

- Heat transfer between thermal supply pipes and other components is considered adiabatic
- Intermittent source, backup source and STES efficiency are independent of subsystem capacity
- Losses per unit length of thermal supply pipe is independent of pipe capacity
- Intermittent source, backup source and STES specific cost are independent of subsystem capacity
- Energy quality is not considered, working temperatures are assumed to be correct for the transfer and use of energy in all subsystems
- Cost of thermal supply pipe per unit length is independent of pipe capacity
- Costs associated with maintenance, personnel and decommissioning or refurbishment are not considered in economic analysis
- Rebates and incentives are not considered in economic analysis

**Thermodynamic analysis:** The following outlines the equations utilized in thermodynamic analysis of the system shown in Fig. 1.

Energy is supplied to the consumer through an intermittent source and a backup source supply chain (Fig. 1). It is assumed that the intermittent source supply chain is capable of providing thermal energy to the consumer at a rate equivalent to the monthly average rate of energy consumption determined through RETScreen. The backup supply chain provides thermal energy to the consumer only under peak load conditions that are beyond the monthly average rate of energy consumption by the consumer. Note that, in RETScreen, consumer peak load data are excluded from that used for calculation of the average consumer loads. Therefore, the annual thermal energy consumption calculated by summing the monthly average rates is less than the total annual consumer load given by RETScreen. The difference between the given and calculated totals represents the amount of thermal energy supplied by the backup supply chain.

The daily amount of thermal energy supplied to the consumer by the intermittent source supply chain, for a given month, ( $Q_{intSC,day,i}$ ) is calculated using the monthly average rate of energy consumption found through RETScreen (Eq. 1).  $i$  ranges from 1 to 12 and represents months January to December, respectively, in all of the following equations:

$$Q_{intSC,day,i} = 24\dot{Q}_{con,i} \quad (1)$$

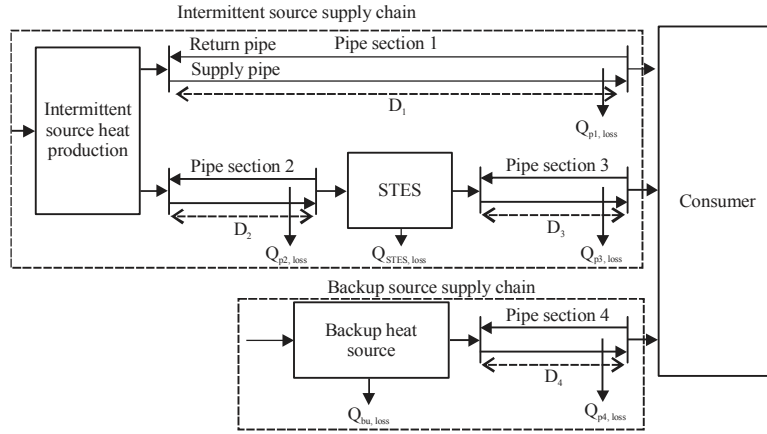


Fig. 1: Basic heating system with intermittent energy source and seasonal thermal energy storage

where  $\dot{Q}_{con,i}$  is the average consumer consumption rate of thermal energy for Month  $i$ .

The annual amount of thermal energy supplied to the consumer by the intermittent supply chain ( $Q_{intSC,annual}$ ) is sum of thermal energy supplied each month of the year:

$$Q_{intSC,annual} = \sum_{i=1}^{12} Q_{intSC,day,i} X_i \quad (2)$$

where  $X_i$  is the number of days in Month  $i$ .

The solar thermal source can only provide thermal energy directly to the consumer when there is daylight available. The thermal energy supplied directly to the consumer each day of Month  $i$  by pipe section one ( $Q_{p1,out,i}$ ) is calculated as:

$$Q_{p1,out,i} = \dot{Q}_{con,i} \bar{n}_i \quad (3)$$

where  $\bar{n}_i$  is the average number of bright sunshine hours in Month  $i$ . When the consumer heating load or number of hours of bright sunshine is zero, the amount of energy being supplied to the consumer, through pipe section one is zero. Locations that experience no bright sunshine during certain times of the year include the northern and southern polar circles. When there is no bright sunshine, heating would need to be supplied by storage or backup subsystems through pipe sections three and four respectively. If there is solar energy available and no consumer load, the thermal energy is sent to storage through pipe section two, as illustrated in Eq. 14.

The amount of thermal energy entering pipe section one each day of Month  $i$  ( $Q_{p1,in,i}$ ) is:

$$Q_{p1,in,i} = Q_{p1,out,i} + Q_{p1,loss,i} \quad (4)$$

where  $Q_{p1,loss,i}$  is the daily heat loss from pipe section one for Month  $i$ .

The annual amount of thermal loss from pipe section one ( $Q_{p1,loss,annual}$ ) is:

$$Q_{p1,loss,annual} = \sum_{i=1}^{12} Q_{p1,loss,i} X_i \quad (5)$$

The daily heat loss from pipe section one is evaluated based on the total length of the pipe in pipe section one ( $L_{p1}$ ), the average heat loss per unit length of pipe ( $q_l$ ) and the amount of time in use each day:

$$Q_{p1,loss,i} = L_{p1} q_l \bar{n}_i \quad (6)$$

When a consumer load exists, the amount of time that pipe section one is in use, each day, is estimated as the average number of daily bright sunshine hours. For periods when the heating load is zero the time that pipe section one is in operation is zero.

The amount of time that pipe section one is in use would be greater than the number of bright sunshine hours. The concept of using hours of bright sunshine implies that solar radiation is available at a constant peak rate for a certain amount of time each day which is equivalent to the amount solar radiation with varying solar radiation rates. In reality, solar radiation rates change over the course of a day and the amount of time when it is actually collected is greater than the number of bright sunshine hours. Therefore, the actual daily thermal loss may be higher than calculated in this model.

The amount of energy supplied to the consumer by pipe section three each day of Month  $i$  ( $Q_{p3,out,i}$ ) is:

$$Q_{p3,out,i} = Q_{intSC,day,i} - Q_{p1,out,i} \quad (7)$$

When the amount of energy being introduced, by the intermittent source, is less than the consumer load and thermal loss from pipe section one, combined, energy is extracted from the STES and delivered to the consumer through pipe three. The amount of thermal energy entering pipe section three each day of Month  $i$  ( $Q_{p3,int,i}$ ) is:

$$Q_{p3,in,i} = Q_{p3,out,i} + Q_{p3,loss,i} \quad (8)$$

where  $Q_{p3,loss,i}$  is the daily heat loss from pipe section three for Month  $i$ .

The daily heat loss from pipe section three is evaluated based on the total length of the pipe in pipe section three ( $L_{p3}$ ):

$$Q_{p3,loss,i} = L_{p3} q_i (24 - \bar{n}_i) \quad (9)$$

The amount of time in use each day is estimated as the difference between the number of hours in a day and the number of hours of bright sunshine.

The annual amount of thermal loss from pipe section three ( $Q_{p3,loss,annual}$ ) is:

$$Q_{p3,loss,annual} = \sum_{i=1}^{12} Q_{p3,loss,i} X_i \quad (10)$$

The amount of thermal energy entering pipe section three annually ( $Q_{p3,in,annual}$ ) is:

$$Q_{p3,in,annual} = \sum_{i=1}^{12} Q_{p3,in,i} X_i \quad (11)$$

The heat transfer processes between the STES subsystem and pipe sections two and three are assumed adiabatic. The amount of thermal energy entering and exiting the STES subsystem is equal to the annually amount of heat exiting pipe section two and entering pipe section three, respectively. The amount of energy fed to the STES subsystem by pipe section two annually ( $Q_{p2,out,annual}$ ) is:

$$Q_{p2,out,annual} = Q_{p3,in,annual} / \eta_{STES} \quad (12)$$

where  $\eta_{STES}$  is the STES thermal efficiency.

The annual amount of heat lost from the STES subsystem is calculated as:

$$Q_{STES,loss,annual} = Q_{p2,out,annual} - Q_{p3,in,annual} \quad (13)$$

The accumulation of thermal energy in the STES system for each month ( $\Delta E_{STES,i}$ ) is calculated as:

$$\Delta Q_{STES,i} = Q_{p2,out,i} - [Q_{p3,in,i} + Q_{p2,out,i}(1 - \eta_{STES})] \quad (14)$$

where  $Q_{p2,out,i}$  and  $Q_{p3,in,i}$  represent the amount of thermal energy entering and exiting the STES subsystem during Month  $i$ , respectively.

The maximum amount of accumulated energy in storage system, throughout the year, represents the capacity of the subsystem. It is calculated as the sum of positive accumulation that occurs in consecutive months. The volume of the STES is utilized for cost analysis and is calculated as the product of the storage capacity and heat capacity of the storage media.

The energy from the intermittent source has two possible paths to follow upon entering the system; through pipe sections one and two. The daily amount of thermal energy supplied to the system by the intermittent source is:

$$Q_{int,out,i} = Q_{p1,in,i} + Q_{p2,in,i} \quad (15)$$

where  $Q_{p2,in,i}$  is the amount of thermal energy entering pipe section two each day of Month  $i$ .

When the amount of energy being introduced by the intermittent source is greater than the consumer load and thermal loss from pipe section one, combined, energy is supplied to the STES subsystem through pipe section two. When the consumer load is zero, the entire thermal energy being produced by the intermittent source is directed to storage.

The annual amount of thermal energy exiting pipe section two is determined through analysis of the STES subsystem. The amount of thermal energy exiting pipe section two must be enough to charge the STES subsystem with sufficient energy to cover the consumer loads that are supplied by the STES subsystem and the thermal losses from the STES. The annual amount of thermal energy exiting pipe section two is the sum of thermal energy exiting each month of the year and is calculated as:

$$Q_{p2,out,annual} = \sum_{i=1}^{12} Q_{p2,out,i} X_i \quad (16)$$

The amount of thermal energy exiting pipe section two each day of Month  $i$  ( $Q_{p2,out,i}$ ) is determined through analysis of the intermittent source (Eq. 15) and the thermal loss from the pipe section each day of the month ( $Q_{p2,loss,i}$ ):

$$Q_{p2,out,i} = Q_{p2in,i} - Q_{p2,loss,i} \quad (17)$$

To assure energy balance in the system, the summation of the output of pipe section two, for months 1 through 12, must equal annual output found in Eq. 12.

The thermal loss from pipe section two each day of the Month  $i$  is:

$$Q_{p2,loss,i} = L_{p2} q_i \bar{\Pi}_1 \quad (18)$$

where  $L_{p2}$  is total length of the pipe in pipe section two. Pipe section two can only be used when there is energy being introduced to the system by the intermittent source that is not being sent directly to the consumer. For simplification, cases involving simultaneous supply of energy from the intermittent source to the consumer (through pipe section one) and storage (through pipe section two) are ignored in this study. The amount of time in operation is assumed to be the number of bright sunshine hours per day if there is energy available. If no energy is available to be sent to the STES system through pipe section two the thermal losses are set to zero.

The annual amount of thermal loss from pipe section two ( $Q_{p2,loss,annual}$ ) is:

$$Q_{p2,loss,annual} = \sum_{i=1}^{12} Q_{p2,loss,i} X_i \quad (19)$$

The daily amount of thermal energy supplied to the system by the intermittent source (solar) subsystem for Month  $i$  ( $Q_{int,out,i}$ ) is:

$$Q_{int,out,i} = \bar{\Pi}_{1,i} A_{collectors} \eta_{int} \quad (20)$$

where  $\bar{\Pi}_{1,i}$  is the monthly average daily radiation on a tilted surface,  $A_{collectors}$  is the total area of the solar collectors and  $\eta_{int}$  is the efficiency of the solar collectors.

The annual amount of thermal energy supplied to the system by the intermittent subsystem ( $Q_{int,out,annual}$ ) is:

$$Q_{int,out,annual} = \sum_{i=1}^{12} Q_{int,out,i} X_i \quad (21)$$

The annual amount of heat that is supplied to the system by the intermittent source is also the sum of thermal energy supplied to the consumer by the intermittent supply chain, the heat loss from pipe sections one to three and the heat loss from the STES subsystem annually:

$$Q_{int,out,annual} = Q_{intSC,annual} + Q_{p1,loss,annual} + Q_{p2,loss,annual} + Q_{p3,loss,annual} + Q_{STES,loss,annual} \quad (22)$$

The amount of thermal energy supplied to the consumer by the backup supply chain ( $Q_{p4,out,annual}$ ) is the difference between the total amount of thermal energy consumed annually provided by RETScreen and the annual amount of thermal energy supplied to the consumer by the intermittent supply chain:

$$Q_{p4,out,annual} = Q_{con,annual} - Q_{intSC,annual} \quad (23)$$

The amount of heat entering pipe section four annually ( $Q_{p4,in,annual}$ ) is:

$$Q_{p4,in,annual} = Q_{p4,out,annual} + Q_{p4,loss,annual} \quad (24)$$

where  $Q_{p4,loss,annual}$  is the annual thermal loss from pipe section four.

Given the assumption of adiabatic heat transfer between pipe sections and subsystems, the amount of energy that is used by the backup source for heat production ( $Q_{BU,in,annual}$ ) is calculated using the annual amount of thermal energy entering pipe section four and the backup subsystem efficiency ( $\eta_{BU}$ ):

$$Q_{BU,in,annual} = Q_{p4,in,annual} / \eta_{BU} \quad (25)$$

The energy consumed by the backup source can be in different forms such as fossil fuel or electricity.

To determine the maximum capacity of the backup system, the peak rate of thermal energy supplied to the consumer ( $\dot{Q}_{p4,out,peak}$ ) is taken as the difference between the peak rate of thermal energy consumption ( $\dot{Q}_{con,peak}$ ) and the highest monthly average rate of energy consumption of the consumer seen throughout the year ( $\dot{Q}_{con,i,max}$ ) provided by RETScreen:

$$\dot{Q}_{p4,out,peak} = \dot{Q}_{con,peak} - \dot{Q}_{con,i,max} \quad (26)$$

The peak rate of thermal energy entering pipe section four represents the peak rate of thermal energy being introduced to the system by the backup subsystem. The peak rate of thermal energy entering pipe section four ( $Q_{p4,in,peak}$ ) is:

$$\dot{Q}_{p4,in,peak} = \dot{Q}_{p4,out,peak} + L_{p4} q_l \quad (27)$$

where  $L_{p4}$  is the total length of piping in pipe section four.

In order to maintain energy balance in the analysis, equations 1-27 must be solved simultaneously.

**Solar analysis:** The average number of hours of bright sunshine for each month is estimated through the use of the following equations<sup>14,15,16</sup>:

$$\frac{\bar{H}_i}{\bar{H}_{0,i}} = a_i + b_i \left( \frac{\bar{n}_i}{\bar{N}_i} \right) \quad (28)$$

where  $\bar{H}_i$  is the monthly average daily radiation on a horizontal surface,  $\bar{H}_{0,i}$  is the monthly average of daily extraterrestrial radiation on a horizontal surface,  $\bar{n}_i$  is the average number of hours of bright sunshine,  $\bar{N}_i$  is the average of the maximum possible hours of bright sunshine and  $a_i$  and  $b_i$  are regression coefficients for Month  $i$ <sup>14,16</sup>.

The regression coefficients for each month are calculated as:

$$a_i = -0.309 + 0.539 \cos \phi - 0.0693 E_0 + 0.290 \left( \frac{\bar{n}_i}{\bar{N}_i} \right) \quad (29)$$

$$b_i = 1.527 - 1.027 \cos \phi - 0.0926 E_0 - 0.359 \left( \frac{\bar{n}_i}{\bar{N}_i} \right) \quad (30)$$

where  $\phi$  is the latitude of the location and  $E_0$  is the elevation of the location above sea level in kilometers<sup>14</sup>.

The monthly average of daily extraterrestrial radiation on a horizontal surface during Month  $i$  is:

$$\bar{H}_{0,i} = \left( \frac{24}{\pi} \right) I_{sc} \left[ 1 + 0.033 \cos \frac{360n}{365} \right] (\cos \phi \cos \delta \sin \omega_s + \omega_s \sin \phi \sin \delta) \quad (31)$$

where  $I_{sc}$  is the solar constant,  $n$  is the day of the year that represents the middle day of Month  $i$ ,  $\delta$  is the declination and  $\omega_s$  is the monthly mean sunrise hour angle for the location.

The average of the maximum possible hours of bright sunshine for Month  $i$  calculated as:

$$\bar{N}_i = \left( \frac{2}{15} \right) \omega_s \quad (32)$$

**Economic analysis:** The following outlines the equations utilized in economic analysis of the system shown in Fig. 1.

The capital cost of each pipe section is dependent on the length total length of piping in the section including supply and return and specific cost of piping per unit length:

$$CC_{p,j} = L_{p,j} SC_{p,j} \quad (33)$$

where  $CC_{p,j}$  is the capital cost,  $L_{p,j}$  is the length and  $SC_{p,j}$  is the specific cost of pipe section  $j$ . Note that  $j$  ranges from one through four depending on pipe section.

The capital cost of all piping in the system ( $CC_p$ ) is:

$$CC_p = \sum_{j=1}^4 CC_{p,j} \quad (34)$$

The capital cost of the STES is dependent on the volume of the STES subsystem and the specific cost of STES storage per unit volume:

$$CC_{STES} = V_{STES} SC_{STES} \quad (35)$$

where  $CC_{STES}$  and  $SC_{STES}$  are the capital cost and specific cost of the STES subsystem, respectively.

Solar thermal collectors are used in the intermittent source subsystem for this study. The capital cost of the solar collectors ( $CC_{int}$ ) is dependent on the total solar collector area and the specific cost of the solar collectors per unit area ( $SC_{collector}$ ):

$$CC_{int} = A_{collectors} SC_{collector} \quad (36)$$

The capital cost of the backup subsystem ( $CC_{BU}$ ) is determined using the backup subsystem capacity and specific cost of the backup subsystem ( $SC_{BU}$ ). The capacity of the backup system is equal to the maximum rate of heat entering pipe section four:

$$CC_{BU} = \dot{Q}_{p4, \text{in, peak}} SC_{BU} \quad (37)$$

Capital cost of the entire heating system is the total of capital costs associated with each subsystem:

$$CC_{system} = CC_{STES} + CC_{int} + CC_{BU} + CC_p \quad (38)$$

Operational costs of the system includes only the cost of fuel consumed by the backup subsystem in this study. The annual cost of fuel calculated as:

$$OC_{BU} = Q_{BU, \text{in, annual}} FC_{BU} \quad (39)$$



where  $OC_{BU}$  is the annual operating cost of the system and  $FC_{BU}$  is the specific fuel cost of the fuel.

The total cost of the system over its lifetime ( $LC_{system}$ ) is:

$$LC_{system} = C_{system} + (OC_{BU}P) \quad (40)$$

where P is the lifetime of the system in years.

**Environmental analysis:** The following outlines the equations utilized in environmental analysis of the system shown in Fig. 1.

There are little to no  $CO_2$  emissions associated with the operation of the solar intermittent sources, STES or pipe subsystems. Emissions associated with these subsystems would mostly arise from the construction, installation, decommissioning and refurbishment of the systems. In order to fully understand the emissions, a lifecycle assessment would need to be completed. In the present study, only  $CO_2$  emissions derived from the fuel consumed by the backup source is considered. In the case of a combustion-based backup system, the emissions would be direct and depend on the fuel. For backup systems utilizing electricity the emissions would be indirect and depend on the emissions from the local power generating stations.

The annual emissions of the system are quantified in mass of  $CO_2$  emitted per year:

$$m_{CO_2,annual} = Q_{BU,in,annual} EI_{fuel} \quad (41)$$

where  $m_{CO_2,annual}$  is the mass of  $CO_2$  emitted annually and  $EI_{fuel}$  is the emission intensity of the fuel.

The total amount of emissions over the lifetime of the system ( $m_{CO_2,lifetime}$ ) is calculated as:

$$m_{CO_2,lifetime} = m_{CO_2,annual} \times X \quad (42)$$

## SIMULATION INPUTS

In the present study, the consumer is assumed to be a single residential building with a floor area of 180  $m^2$  located in Ottawa, Ontario, Canada. Heating load and solar radiation data are taken from RETScreen 4 with the Ottawa International Airport set as the location.

The peak heating load depends on the design of a building, its application and its location. The peak heating load for residential homes in Ottawa ranges from 0.055-0.085  $kW/m^2$ <sup>17</sup>. A value of 0.070  $kW/m^2$  is utilized for the peak heating load.

Multiple technologies exist for each of the subsystems. The subsystem efficiencies initially utilized are assumed to be the mean values of the upper and lower limits found in the literature for each subsystem. This approach allows for thermodynamic analysis to be performed with limited data. To improve accuracy, multiple systems should be analyzed and weighted averages developed to identify typical subsystem efficiency values.

For this study, the intermittent source is solar which produces thermal energy in liquid-based solar thermal collectors. The slope and azimuth of the solar collectors are 45 and 0 degrees, respectively. Solar collector efficiency depends on the design, inlet and outlet temperatures of the heat transfer fluid and the surrounding temperature. Solar thermal technologies have solar collector efficiencies of 25.0-70.0%<sup>18,19</sup>. A mean solar collector efficiency of 47.5% is utilized.

Underground Thermal Energy Storage (UTES) is utilized for the STES system. UTES efficiency depends on the technology, size of storage, storage media and amount of insulation and duration of storage. Typically, UTES systems have an efficiency between 40.0 and 87.0%<sup>20-24</sup>. Initially, an average value of 63.5% is used for STES efficiency.

The backup system is used to supply the consumer with thermal energy at a rate higher than the average consumer load. The backup source is a natural gas fired boiler. Natural gas boilers have efficiency values ranging from 75.0-97.0%<sup>25,26</sup>. The backup source efficiency is set to 86.0%.  $CO_2$  emission intensity natural gas combustion ranges from 0.19-0.21  $kg\ CO_2/kWh_{th}$ <sup>27-29</sup>. An average value of 0.20  $kg\ CO_2/kWh_{th}$  is applied.

The STES is located equidistant from intermittent source and consumer. The backup system is the same distance from the consumer as the storage. Each thermal supply pipe section is comprised of a supply and return pipe, and therefore the length of pipe in each pipe section is taken as double the distance between subsystems. The distance each pipe section must cover is specified in Table 1. Losses from the thermal supply piping is dependent on pipe design, amount of insulation, internal flow conditions, fluid temperature and surrounding temperature. Typically, the thermal losses from thermal supply piping, for the feed and return pipes combined, ranges from 0.002-0.013  $kW/m_{pipe}$ <sup>30-32</sup>. A unit heat loss rate of 0.002  $kW/m_{pipe}$  is typical of a double pipe design with a high degree of insulation and 0.013  $kW/m_{pipe}$  is representative of a single pipe design with little insulation. A value of 0.0075  $kW/m_{pipe}$  is utilized for the base study.

The specific cost of liquid based solar thermal collectors depends on the technology and manufacturer of the collectors. It is found that the specific cost of solar thermal collectors, in Canada, range from 125.0-1000 \$/m<sup>2</sup> 33,34. A mean value of 562.5 \$/m<sup>2</sup> is utilized in this study. Monetary units in this paper are in Canadian dollars (CAD) or Canadian cents.

The specific cost of a natural gas boiler ranges from 35.00-200.0 \$/kW<sub>th</sub>. A specific cost of 117.5 \$/kW<sub>th</sub> is utilized in the study. The specific cost of natural gas depends on the location and supplier. The average natural gas price for January 1, 2016, in Ontario is found to be between 9.48 and 18.70 ¢/m<sup>3</sup> including storage and transportation charges<sup>35</sup>. This is equivalent to a range of 1.00-1.98 ¢/kWh using the lower heating value of natural gas. An average specific cost of 1.49 ¢/kWh for natural gas is employed.

The capital cost of the thermal supply piping depends on the pipe dimensions, design (single-, twin- or multi-pipe) amount of insulation and method of installation. It is found that the specific cost of thermal supply piping typically ranges from 75.0 to 650.0 \$/m. A mean value of 362.5 \$/m is utilized for all pipe sections. Each pipe section may not be of the same size and design. Ideally, the cost of each piping in each pipe section would be found using a specific cost that is more relevant to pipe design in each pipe section.

The capital cost of UTES depends on the technology, storage capacity, storage media, degree of insulation and system location. The specific cost varies between 85.0 and 520 \$/m<sup>3</sup> water eq. 10,36 and a mean value of 302.5 \$/m<sup>3</sup> water eq. is utilized. To determine the volume of the STES subsystem, it is assumed that water is the storage media with a mean heat capacity of 70.0 kWh/m<sup>3</sup> 36.

Using the average values outlined above and assuming a lifecycle of 20 years, the values for total capital cost annual running cost, lifetime cost, annual CO<sub>2</sub> emissions, lifetime CO<sub>2</sub> emissions and solar fraction are determined. The results are summarized in Table 2.

## RESULTS AND DISCUSSION

The effects of varying different subsystem parameters on the cost and CO<sub>2</sub> emissions associated with a heating system with STES are investigated using parametric studies. The subsystem parameters that are investigated include consumer load, STES subsystem efficiency, intermittent and backup source efficiency and thermal supply network losses per unit length.

**Effect of varying peak consumer load:** To quantify the significance of peak consumer load on system capital cost and

annual CO<sub>2</sub> emissions, analysis is conducted in which consumer load is varied from 0.055-0.085 kW/m<sup>2</sup>. Varying the peak consumer load results in a variation in the monthly average rate of thermal energy consumption throughout the year and the total amount of energy consumed annually with the presented method and model. The investigation is performed for three scenarios: high, low and average cost where the high, low and average values for the subsystem capital costs are applied. Subsystem efficiency and pipe loss values remain constant.

Table 3 illustrates the effect of peak consumer load on system capital cost. It is shown that the capital cost increases with increased peak load. As the peak load increases, the subsystem capacities also increase, which results in higher subsystem capital costs. When the cost of the subsystems is low, there is greater change in the system capital cost over the range of peak heating load. For a 42.9% increase of in peak heating load, the capital cost increases by a percent difference of 14.6, 13.0 and 12.7% for low, average and high cost scenarios, respectively.

The cost of the thermal supply pipes have the highest capital cost and contribute the most to the system capital cost, in all scenarios (approximately 56-70%). This is followed by the STES (17-28%), solar source (12-15%) and backup (>1%) subsystems, respectively. In this study, the capital cost of the supply pipes are not dependent on capacity and therefore remain constant as the peak heating load is increased. As the heating load is increased the influence of supply pipe cost on capital cost decreases and the contribution of the other

Table 1: Assumed distances between subsystems

Length	D <sub>1</sub>	D <sub>2</sub>	D <sub>3</sub>	D <sub>4</sub>
Distance (m)	100	50	50	50

Table 2: Calculated results using average system values

Parameter	Value
Total capital cost (CAD)	276,400
Annual fuel cost (CAD)	27
System life cycle cost (CAD)	276,900
Annual CO <sub>2</sub> emissions (kg CO <sub>2</sub> /year)	359.8
Lifetime CO <sub>2</sub> emissions (kg CO <sub>2</sub> )	7,195
Solar fraction (%)	94.9

Table 3: Effect of peak consumer load on system capital cost for low, average and high cost scenarios

Peak consumer load (kW/m <sup>2</sup> )	System capital cost (CAD)		
	Low cost scenario	Average cost scenario	High cost scenario
0.0550	57,370	258,700	459,900
0.0625	59,660	267,500	475,400
0.0700	61,970	276,400	490,800
0.0775	64,270	285,300	506,300
0.0850	66,570	294,100	521,700

subsystems increase. It is found that the increase in STES size creates the greatest change in system capital cost.

If the distances between the subsystems were reduced, there would be a reduction in their associated capital cost. Reducing pipe lengths would also cause a reduction in thermal losses in the system, which in turn may lower the required capacities of the solar, STES and backup subsystems resulting in further reduction in system capital cost. If the backup source was used to provide additional thermal energy to the consumer, beyond peak load operation, the capital cost of the system may be reduced but would also result in increased operational costs and CO<sub>2</sub> emissions.

The annual CO<sub>2</sub> emissions increase linearly, as the peak heating load increases, due to a linear increase in the backup system capacity and fuel consumption. It is found that the annual CO<sub>2</sub> emission vary from 290.9-428.6 kg CO<sub>2</sub>/year in all scenarios, over the range of peak heating loads considered.

**Effect of varying STES (UTES) efficiency on system capital cost:**

The effects of carrying STES, specifically UTES, efficiency on system capital cost are investigated through parametric analysis. UTES efficiency depends on many factors, but to quantify its influence on the system capital cost, the efficiency is varied independent of other parameters. The STES efficiency is varied from 40.0-87.0%. The average subsystem efficiencies, solar availability and building characteristics specified in the simulation inputs section are held constant with the exclusion of STES efficiency. The investigation is performed for the low, average and high cost scenarios.

Table 4 illustrates the effect of STES efficiency on system capital cost. As the STES efficiency increases, the system capital cost decreases. For an increase of 47.0% in STES efficiency, there is a reduction in system capital cost of approximately 8.0, 8.5 and 8.6% for the low, average and high cost scenarios, respectively.

Increasing the STES efficiency results in reduced losses from the STES resulting in a decrease in the amount of thermal energy supplied to the STES subsystem. Changing the amount of energy supplied to the STES subsystem directly affects the solar collector area and capital cost. There is a reduction in solar collector area and solar collector cost of approximately 48.2% for all scenarios. The system capital cost is comprised mostly of the cost of the thermal supply piping and STES subsystems in all cost scenarios, therefore a large reduction in solar collector area does not greatly effect overall capital cost in this study.

The annual CO<sub>2</sub> emissions for all cost scenarios 359.8 kg CO<sub>2</sub>/year and remain constant over the range of STES efficiency values and cost scenarios considered. This is due to a constant solar fraction and backup fuel consumption.

Table 4: Effect of STES efficiency on system capital cost for low, average and high cost scenarios

STES efficiency (%)	System capital cost (CAD)		
	Low cost scenario	Average cost scenario	High cost scenario
40.0	65,640	293,500	521,300
61.0	62,210	277,600	492,900
82.0	60,790	270,700	480,600
87.0	60,580	269,600	478,700

Table 5: Effect of intermittent source efficiency on system capital cost for low, average and high cost scenarios

Intermittent source efficiency (%)	System capital cost (CAD)		
	Low cost scenario	Average cost scenario	High cost scenario
25	69,710	311,200	552,800
45	62,440	278,500	494,600
65	59,650	266,000	472,300
70	59,200	263,900	468,700

**Effect of varying intermittent source (solar collector) efficiency:**

The effects of varying intermittent source, specifically solar thermal, efficiency on system capital cost are investigated through parametric analysis. The intermittent source efficiency is varied from 25.0-70.0%. Other subsystem efficiencies, solar availability and building characteristics specified in the simulation inputs section are held constant. The investigation is performed for low average and high cost scenarios.

The effect of varying intermittent source efficiency on system capital cost is shown in Table 5. The system capital cost decreases with increasing intermittent source efficiency. As the efficiency increases, the solar collector area required to supply the necessary amount of thermal energy to the system decreases. Under the assumption that the price per unit area of solar collector remains constant, the capital cost of the intermittent source subsystem is reduced. Overall, an increase in efficiency of 45.0% results in a reduction in solar collector area of 64.3% and a reduction in system capital cost of and 15.6, 16.7 and 16.5% for the low, average and high cost scenarios, respectively.

**Effect of varying backup source efficiency:**

The effect of varying backup source efficiency on system capital cost, lifecycle cost and life cycle CO<sub>2</sub> emissions are investigated through parametric analysis. The backup source efficiency is varied independent of other parameters. The intermittent source efficiency is varied from 75.0-97.0%. Other subsystem efficiencies, source and building characteristics specified in the simulation inputs section are held constant. The investigation is performed for low, average and high cost scenarios.

Table 6: Effect of backup source efficiency on life cycle cost for low, average and high cost scenarios

Backup source efficiency (%)	Life cycle cost (CAD)		
	Low cost scenario	Average cost scenario	High cost scenario
75	62,380	277,000	491,600
85	62,330	276,900	491,500
95	62,290	276,900	491,500
97	62,280	276,900	491,400

The life cycle cost varies with backup efficiency as a consequence of changing the annual fuel consumption. Table 6 illustrates the effect of backup source efficiency on the life cycle cost. Overall, there is very small variance in the life cycle cost associated with an increase in backup efficiency of 45.0%. There is less than 1% difference in the lifecycle cost over the range of backup efficiency for all cost scenarios, which is a result of the small contribution of the backup system toward the annual consumer load (5.1%). CO<sub>2</sub> emissions vary by 23% over the range of backup efficiency. The backup source efficiency does not affect the capacity or amount of thermal losses in the intermittent source supply chain. If the solar fraction was reduced, the change in life cycle cost and CO<sub>2</sub> emissions would be more predominant.

Overall, the system capital cost is unchanged by variance in backup source efficiency. The capital cost of the low average and high cost scenarios are 61,970, 276,400 and 490,800 CAD, respectively.

Additional studies are required to explore the influence of backup source efficiency in scenarios with reduced solar fractions.

**Effect of varying thermal supply pipe losses:** The effect thermal supply pipe losses on capital cost, running cost and CO<sub>2</sub> emissions are investigated. The thermal supply pipe losses are varied from 0.002-0.013 kW/m<sub>pipe</sub> outlined in the simulation inputs section.

As the thermal supply losses increase, the system capital cost increases. When there are additional losses between the subsystems, the capacity of the other subsystems increase in order to support the consumer load. When the capacity of the subsystems are increased, there is an associated increase in their capital cost. With an increase in supply pipe losses of 147%, there is an increase in system capital cost of approximately 14.8%, for all cost scenarios.

The amount of fuel consumed by the backup subsystem varies with supply pipe losses as the amount of fuel consumed by the backup system varies. The variation is limited due to the low amount of energy being supplied by the backup system

to the consumer. The annual fuel cost varies by 14.5% over the range of supply pipe losses, which represents less than 1% of the system life cycle cost. The annual CO<sub>2</sub> emissions also vary by 14%, from 332 to 388 kg year<sup>-1</sup>. It is expected that the results will expand the knowledge base and also will enhance other studies on related topics, which include investigations of the underground energy storage<sup>37,38</sup>, solar energy<sup>39</sup>, and environmental impact associated with ground processes<sup>40,41</sup>.

## CONCLUSIONS

A method to analyze a heating system with seasonal thermal energy storage is developed and applied to perform parametric analyses of a system that uses solar thermal energy, a natural gas backup and a seasonal, underground thermal energy storage, in order to identify the significance of various subsystem parameters on system CO<sub>2</sub> emissions and economics. The analysis provides insights into the importance of various subsystem characteristics for a system with these particular subsystem components. The main conclusions drawn from the results follow:

- Varying the heating load significantly affects the system capital cost. Over the range of peak heating load values, the system with the average cost considerations changes by 14%. Increasing the underground thermal energy storage cost contributes the most to the change in capital cost followed by the solar thermal collector costs.
- Increasing the underground thermal energy storage efficiency, independent of its capital cost, decreases the capital cost for the considered system by 8% over the range of values considered. The decrease in capital cost is not great compared to changing other subsystem characteristics over their typical ranges. Increasing the seasonal thermal energy storage efficiency decreases the solar collector area, but the overall effect is low due to the low contribution of the solar collectors to the capital cost.
- In all studies, the backup source capital cost contributes little to the total capital cost considering the system layout and assumptions. This is due to the high solar fraction and low backup source capacity.
- The subsystem characteristics that affect CO<sub>2</sub> emissions are consumer load, backup source efficiency and thermal supply pipe losses. In this study, variations in the characteristics associated with the intermittent supply chain have no effect on CO<sub>2</sub> emissions. Additional investigations are required to explore the effects of a system with different solar fractions.

- Overall, the peak heating load per unit area of floor space has the greatest effect on CO<sub>2</sub> emissions over the typical ranges of subsystem characteristics considered. In this study, buildings with low peak loads should be utilized in order to reduce emissions.

To improve the understanding of subsystem characteristics on overall system economics and CO<sub>2</sub> emissions, the study should be conducted with variations in subsystem technologies, solar collector orientation, consumer type, location (varying heating load and solar conditions) and solar fraction.

Numerous simplifying assumptions were made to develop the approach and to complete analysis, which introduce limitations and inaccuracies. Limitations identified throughout the study should be addressed in development of more advanced models.

### **SIGNIFICANCE STATEMENT**

The use of intermittent thermal energy sources (e.g., solar), in combination with seasonal thermal energy storage, for space heating may be advantageous to conventional heating systems. Typically heating systems with thermal storage are customized and require complex analysis. This study presents a method to analyze heating systems with seasonal thermal energy storage that has reduced complexity compared to many available methods. Studies are conducted to increase understanding of the effects of various subsystems (and their characteristics and efficiencies) on the performance, economic and environmental aspects of a heating system, with seasonal storage. The results provide insights into the importance of various subsystem characteristics on system operation, costs and carbon dioxide emissions. The results and trends developed can aid design and feasibility studies.

### **ACKNOWLEDGMENTS**

The authors kindly acknowledge financial support provided by the Natural Sciences and Engineering Research Council of Canada.

### **REFERENCES**

1. Pinnau, S. and C. Breitkopf, 2015. Determination of thermal energy storage (TES) characteristics by fourier analysis of heat load profiles. *Energy Convers. Manage.*, 101: 343-351.
2. Kapsalaki, M., V. Leal and M. Santamouris, 2012. A methodology for economic efficient design of net zero energy buildings. *Energy Build.*, 55: 765-778.
3. Pavlov, G.K. and B.W. Olesen, 2012. Thermal energy storage-a review of concepts and systems for heating and cooling applications in buildings: Part 1-Seasonal storage in the ground. *HVAC&R Res.*, 18: 515-538.
4. Dincer, I. and M.A. Rosen, 2011. *Thermal Energy Storage: Systems and Applications*. 2nd Edn., John Wiley and Sons, New York, USA., ISBN: 9781119956624, Pages: 620.
5. Haeseldonckx, D., L. Peeters, L. Helsen and W. D'haeseleer, 2007. The impact of thermal storage on the operational behaviour of residential CHP facilities and the overall CO<sub>2</sub> emissions. *Renew. Sustain. Energy Rev.*, 11: 1227-1243.
6. Pavlov, G.K. and B.W. Olesen, 2011. Seasonal ground solar thermal energy storage-review of systems and applications. *Proceedings of the ISES Solar World Congress, August 28-September 2, 2011, Kassel, Germany*.
7. Sharma, A., V.V. Tyagi, C.R. Chen and D. Buddhi, 2009. Review on thermal energy storage with phase change materials and applications. *Renew. Sustain. Energy Rev.*, 13: 318-345.
8. Gaine, K. and A. Duffy, 2010. A life cycle cost analysis of large-scale thermal energy storage technologies for buildings using combined heat and power. *Proceedings of the Renewable Energy Conference, June 7-8, 2010, Trondheim, Norway*.
9. Novo, A.V., J.R. Bayon, D. Castro-Fresno and J. Rodriguez-Hernandez, 2010. Review of seasonal heat storage in large basins: Water tanks and gravel-water pits. *Applied Energy*, 87: 390-397.
10. Schmidt, T., D. Mangold and H. Muller-Steinhagen, 2004. Central solar heating plants with seasonal storage in Germany. *Solar Energy*, 76: 165-174.
11. Dincer, I. and S. Dost, 1996. A perspective on thermal energy storage systems for solar energy applications. *Int. J. Energy Res.*, 20: 547-557.
12. Sweet, M.L. and J.T. McLeskey Jr., 2012. Numerical simulation of underground Seasonal Solar Thermal Energy Storage (SSTES) for a single family dwelling using TRNSYS. *Solar Energy*, 86: 289-300.
13. Natural Resources Canada, 2016. RETScreen. Natural Resources Canada. <http://www.nrcan.gc.ca/energy/software-tools/7465>
14. Tiwari, G.N., 2002. *Solar Energy: Fundamentals, Design, Modeling and Applications*. 1st Edn., Narosa Publishing House, New Delhi, India.
15. Kumar, R. and L. Umanand, 2005. Estimation of global radiation using clearness index model for sizing photovoltaic system. *Renew. Energy*, 30: 2221-2233.
16. Sen, Z., 2008. *Solar Energy Fundamentals and Modeling Techniques: Atmosphere, Environment, Climate Change and Renewable Energy*. Springer, London, ISBN: 9781848001343, Pages: 276.
17. Natural Resources Canada, 2012. RETScreen CHP (cogeneration) project model: Tools and other algorithms. Natural Resources Canada, Ottawa, Canada.

18. Chow, T.T., 2010. A review on photovoltaic/thermal hybrid solar technology. *Applied Energy*, 87: 365-379.
19. Kumar, R. and M.A. Rosen, 2011. A critical review of photovoltaic-thermal solar collectors for air heating. *Applied Energy*, 88: 3603-3614.
20. Rezaie, B., B.V. Reddy and M.A. Rosen, 2015. Exergy analysis of thermal energy storage in a district energy application. *Renew. Energy*, 74: 848-854.
21. Schout, G., B. Drijver, M. Gutierrez-Neri and R. Schotting, 2014. Analysis of recovery efficiency in high-temperature aquifer thermal energy storage: A Rayleigh-based method. *Hydrogeol. J.*, 22: 281-291.
22. Sibbitt, B., D. McClenahan, R. Djebbar, J. Thornton, B. Wong, J. Carriere and J. Kokko, 2012. The performance of a high solar fraction seasonal storage district heating system-five years of operation. *Energy Proc.*, 30: 856-865.
23. Yapparova, A., S. Matthai and T. Driesner, 2014. Realistic simulation of an aquifer thermal energy storage: Effects of injection temperature, well placement and groundwater flow. *Energy*, 76: 1011-1018.
24. Xu, J., R.Z. Wang and Y. Li, 2014. A review of available technologies for seasonal thermal energy storage. *Solar Energy*, 103: 610-638.
25. Ghafghazi, S., T. Sowlati, S. Sokhansanj and S. Melin, 2010. Techno economic analysis of renewable energy source options for a district heating project. *Int. J. Energy Res.*, 34: 1109-1120.
26. Wu, K.K., Y.C. Chang, C.H. Chen and Y.D. Chen, 2010. High-efficiency combustion of natural gas with 21-30% oxygen-enriched air. *Fuel*, 89: 2455-2462.
27. IPCC., 2006. 2006 IPCC guidelines for national greenhouse gas inventories. Institute for Global Environmental Strategies, Intergovernmental Panel on Climate Change, USA.
28. Natural Resources Canada, 2013. CO<sub>2</sub> emission factors. Natural Resources Canada. <http://www.nrcan.gc.ca/energy/efficiency/industry/technical-info/benchmarking/canadian-steel-industry/5193>
29. U.S Energy Information Administration, 2015. How much carbon dioxide is produced when different fuels are burned? <https://www.eia.gov/tools/faqs/faq.cfm?id=73&t=11>.
30. Kristjansson, H. and B. Bohm, 2006. Advanced and traditional pipe systems: Optimum design of distribution and service pipes. Proceedings of the 10th International Symposium on District Heating and Cooling, September 3-5, 2006, Hanover, Germany.
31. Olsen, P.K., C.H. Christiansen, M. Hofmeister, S. Svendsen and J.E. Thorsen, 2014. Guidelines for low-temperature district heating. Deliverable of Danish EUDP 2010-II Project, Danish Energy Agency, Denmark.
32. Rosa, A.D., H. Li and S. Svendsen, 2011. Method for optimal design of pipes for low-energy district heating, with focus on heat losses. *Energy*, 36: 2407-2418.
33. Djebbar, R., 2013. Survey of active solar thermal collectors, industry and markets in Canada (2012). Natural Resources Canada, Ottawa, Canada.
34. Rad, F.M., A.S. Fung and W.H. Leong, 2013. Feasibility of combined solar thermal and ground source heat pump systems in cold climate, Canada. *Energy Build.*, 61: 224-232.
35. Ontario Energy Board, 2016. Natural gas rate updates. <http://www.ontarioenergyboard.ca/OEB/Consumers/Natural+Gas/Natural+Gas+Rates>.
36. Schmidt, T. and O. Miedaner, 2012. Solar district heating guidelines. Final Report, Solar District Heating, European Union. [http://solar-district-heating.eu/Portals/0/Factsheets/SDH-WP3-D31-D32\\_August2012.pdf](http://solar-district-heating.eu/Portals/0/Factsheets/SDH-WP3-D31-D32_August2012.pdf)
37. Sliwa, T., M.A. Rosen and Z. Jezuit, 2014. Use of oil boreholes in the Carpathians in geoeconomic systems: Historical and conceptual review. *Res. J. Environ. Sci.*, 8: 231-242.
38. Tolmie, R. and M.A. Rosen, 2015. Storing exergy in the ground: An effective use of the environment. *Res. J. Environ. Sci.*, 9: 66-73.
39. Ataei, A., A. Haji-Mola-Ali Kani, R. Parand and M. Raoufinia, 2009. Optimum design of a photovoltaic reverse-osmosis system for Persian Gulf water solar desalination. *Res. J. Environ. Sci.*, 3: 414-426.
40. Al-Jilil, S.A., 2015. Characterization and application of Bentonite clay for lead ion adsorption from wastewater: Equilibrium and kinetic study. *Res. J. Environ. Sci.*, 9: 1-15.
41. Sadeghi, S., B. Shahmoradi and A. Maleki, 2015. Estimating methane gas generation rate from Sanandaj city landfill using LANDGEM software. *Res. J. Environ. Sci.*, 9: 280-288.